PHYSICAL REVIEW B **84**, 241405(R) (2011)

Noble gases on metal surfaces: Insights on adsorption site preference

De-Li Chen,[1,2] W. A. Al-Saidi,[2] and J. Karl Johnson[1,2,*]

[1]*National Energy Technology Laboratory, Pittsburgh, Pennsylvania 15236, USA*

[2]*Department of Chemical and Petroleum Engineering, University of Pittsburgh, Pittsburgh, Pennsylvania 15261, USA*

(Received 4 November 2011; published 19 December 2011)

We use a nonlocal van der Waals density functional (vdW-DF) approach to reexamine the problem of why noble gases are experimentally observed to adsorb on low-coordination atop sites rather than on high-coordination hollow sites for several different metal surfaces. Previous calculations using density functional theory (DFT) within the local density approximation (LDA) ascribed the site preference to reduced Pauli repulsion at atop sites, largely due to reduced exchange repulsion within LDA-DFT. In contrast, our vdW-DF calculations show that site preference is not due to differences in the exchange repulsion at all, but rather the result of a delicate balance between the electrostatic and kinetic energies; surprisingly, exchange-correlation energies play a negligible role in determining site preference. In contrast to previous calculations, we find that experimental results cannot be explained in terms of binding energy differences between atop and hollow sites. Instead, we show that the hollow sites are transition states rather than minima on the two-dimensional potential energy surface, and therefore not likely to be observed in experiments. This phenomenon is quite general, holding for close-packed and non-close-packed metal surfaces. We show that inclusion of nonlocal vdW interactions is crucial for obtaining results in quantitative agreement with experiments for adsorption energies, equilibrium distances, and vibrational energies.

DOI: 10.1103/PhysRevB.84.241405 PACS number(s): 68.43.−h

The adsorption of noble gas atoms on various metal surfaces has been studied extensively for many years.[1–3] These systems are of interest because they are prototypical of physical adsorption, where the primary interaction between the adsorbate and substrate consists of a balance between long-range van der Waals (vdW) attraction and short-range Pauli repulsion. Precise determination of the adsorption sites for noble gas atoms on metal surfaces from theory is problematic because the interactions are so weak and are therefore difficult to compute from approximate first-principles approaches that cannot account accurately for electron correlation effects. Experimental site preference determination has also proved difficult. For example, initial spin-polarized low-energy electron diffraction (LEED) studies[4,5] of Xe/Pt(111) and Xe/Pd(111) with $(\sqrt{3} \times \sqrt{3})R30^\circ$ structure indicated a hollow site adsorption preference. However, later experimental work reflects a consensus that only atop site adsorption is observed for a variety of systems, including Xe/Pt(111) and Xe/Pd(111),[6–8] Cu(111),[9] and Ru(0001).[10] This preference for low-coordination sites also extends to more open, non-close-packed surfaces, as shown for Xe/Cu(110), where the Xe atoms are localized on the top of rows rather than the troughs.[11] These experimental findings were surprising because high-coordination sites are typically favored for systems governed by physical adsorption forces.

Given that the gas/surface interaction in these systems is expected to be dominated by weak vdW interactions, one might expect that the use of model pair potentials such as the Lennard-Jones (LJ) potential would give a reasonably accurate description of the physics of adsorption.[12] However, LJ potentials predict a preference for high-coordination site adsorption,[13] which is contradictory to the experimental findings. Standard density functional theory (DFT) methods do not properly account for long-range electron correlation (dispersion) interactions. However, it has been previously noted that the use of the local density approximation (LDA) in DFT often gives interaction energies for weakly bound systems that are approximately and fortuitously correct,[14] although the form of the interaction potential is incorrect. Therefore, LDA-DFT has been used to describe the adsorption of noble gases on various metal surfaces.[15–18] The generalized gradient approximation (GGA), which is generally considered to be more accurate than LDA, dramatically underestimates the adsorption energies and vibrational energies for noble gas/metal surface systems, and overestimates the equilibrium adsorption distances compared with experimental data.[16,17] Da Silva *et al.* therefore used LDA-DFT calculations to explore the reasons for atop over hollow site adsorption preference.[16–18] They concluded that the dominant reasons that low-coordination sites are favored are that polarization is stronger and Pauli repulsion is weaker on atop sites relative to hollow sites.

Given the well-known limitations of the LDA functional and the recent development of approximate but reasonably accurate methods for including vdW interactions within DFT, here we reevaluate the reasons for rare gas atoms preferring low-coordination adsorption sites. We have used DFT calculations employing the vdW-DF2 functional[19,20] to account for weak interactions in the noble gas/metal surface systems. This approach has been successfully used for other systems involving gas adsorption on metals.[21,22] Our results indicate, in contrast to LDA calculations, that differences in exchange-correlation energies are not the determining factors for the site preference. Also, we show that the difference in energy between the atop and fcc sites is only a few milli-electron-volts. Such small energy differences are, at first glance, not consistent with experimental findings that only atop site adsorption is observed at $T = 80$ K.[23] However, on closer examination we find that hollow sites are actually saddle points of index 2, and not minima on the potential

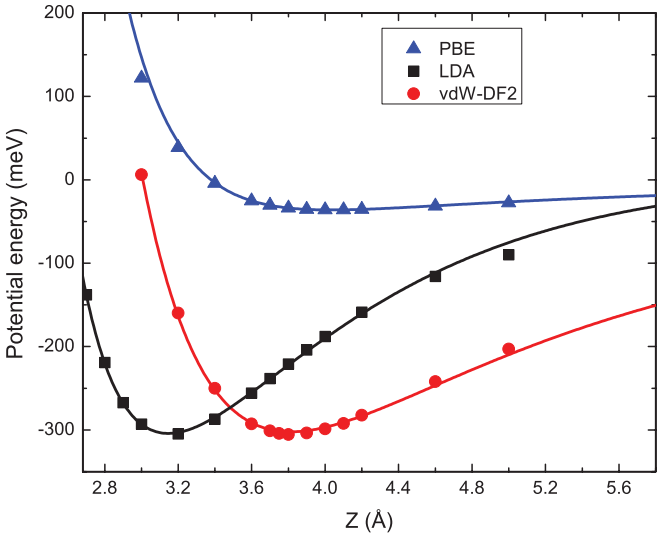

FIG. 1. (Color online) Potential energy for atop adsorption of Xe in the $(\sqrt{3} \times \sqrt{3})R30^\circ$ structure on Pt(111) as a function of the perpendicular distance to the surface (Z) computed from PBE (triangles), LDA (squares), and vdW-DF2 (circles). The curves are fitted to the data using Eq. (1).

energy surfaces (PES). Saddle points of index 1 and 2 have one and two imaginary frequencies, respectively. Therefore, the index 1 saddle point corresponds to a transition state on the PES, where the eigenvector having an imaginary frequency connects two minima (atop sites). The index 2 saddle point is a local maximum on the two-dimensional (2D) PES, having two eigenvectors with imaginary frequencies parallel to the surface. Hence the reason that adsorption at hollow sites is not observed is that these are ephemeral transient states rather than true stable states.

Our vdW-DF2 functional calculations were carried out non-self-consistently using an in-house code that implements the fast Fourier transformation evaluation technique introduced by Román-Pérez and Soler.[24] The charge densities needed for the non-self-consistent vdW-DF2 calculations were computed using the Perdew-Burke-Ernzerhof (PBE) functional[25] with Vienna Ab-initio Simulation Package (VASP).[26] Test calculations indicate that using non-self-consistent electron densities result in about a 15% difference in the nonlocal energies near the potential minimum. The metal surfaces were modeled using a repeated slab of several atomic layers (six to seven layers for different metal surfaces), which were shown to yield converged results. We used a vacuum spacing of 20 Å to mitigate the interactions between the periodic images along the stacking direction of the slab. An energy cutoff of 600 eV was used in all of the calculations, and we employed an $8 \times 8 \times 1$ Monkhorst-Pack grid.

Figure 1 shows the potential energy curves of the Xe $(\sqrt{3} \times \sqrt{3})R30^\circ$ monolayer atop adsorption on Pt(111) computed from LDA, PBE, and vdW-DF2 functionals. Adsorption energies ($E_{\rm ad}$) and equilibrium distances (d) computed from these functionals are compared with experimental data in Table I. We see that values of $E_{\rm ad}$ and d computed from vdW-DF2 are in better agreement with experiments[12,23,27,28] than predictions from any of the other functionals used herein. That the long-range vdW interactions are important can be judged by noting that the PBE functional predicts $E_{\rm ad}$ to be an order of magnitude smaller than experiments and a value of d that is too large. In contrast, LDA gives a value of $E_{\rm ad}$ in fortuitous agreement with experiments, while underestimating d. We computed vibrational energies for the Xe mode perpendicular to the metal surface from a physically motivated potential, which is given by the sum of repulsive and attractive vdW interactions:[12,17]

$$V(Z) = \alpha_1 e^{-\alpha_2 Z} - C_3/(Z - Z_0)^3. \quad (1)$$

The parameters α_1, α_2, C_3, and Z_0 were determined by fitting to the DFT results. The vibrational energy was calculated from $h\nu = h/2\pi\sqrt{k_e/M_{\rm gas}}$, where ν, h, and $M_{\rm gas}$ are the vibrational frequency, Plank's constant, and the mass of the gas atom, respectively. k_e was computed from the second derivative of the potential at the minimum. Again comparing with available experimental data (Table I), the vdW-DF2 vibrational energies are in good agreement with experimental values,[7,29] while LDA overestimates and PBE underestimates $h\nu$.

All of the calculations (LDA, PBE, vdW-DF2) show that atop site is energetically favored over the hollow site. However, the magnitude of the energy difference between atop and hollow adsorption is dramatically different: 38.4, 2.5, and 5.3 meV for LDA, PBE, and vdW-DF2, respectively. The preference for low-coordination sites extends to other metal surfaces, including non-close-packed surfaces, and other noble gases (see Table I); in each case the adsorption energy differences between low and high coordination sites computed from

TABLE I. The calculated adsorption energy ($E_{\rm ad}$, in meV), equilibrium distance (d, in Å), and perpendicular mode vibrational energy ($h\nu$, in meV) of noble gases on various metal surfaces at low-coordination (atop or ridge) sites as computed from LDA, PBE, vdW-DF2, and from experiments. The values in brackets represent the difference in adsorption energies between the fcc and atop sites [trough and ridge sites for Cu(110)]: $E_{\rm diff} = E_{\rm ad}^{\rm fcc} - E_{\rm ad}^{\rm atop}$. The experimental data are from Refs. 5,8,9,11,12,23,27, and 28.

	LDA			PBE			vdW-DF2			Expt		
	$E_{\rm ad}$	d	$h\nu$	$E_{\rm ad}$	d	$h\nu$	$E_{\rm ad}$	d	$h\nu$	$E_{\rm ad}$	d	$h\nu$
Xe/Pt(111), monolayer	−304.8[38.4]	3.2	5.2	−36.1 [2.6]	4.0	1.4	−305.2 [5.2]	3.8	3.6	−270 to −320	3.4	3.5,3.7
Xe/Pd(111), monolayer	−396.3[36.2]	2.9	6.5	−52.1 [6.6]	3.6	2.1	−309.8 [5.3]	3.7	3.4	−320	3.5,3.07,3.61	–
Xe/Cu(111), monolayer	−255.5[7.1]	3.3	3.8	−15.5 [0.1]	4.5	1.1	−269.6 [1.0]	4.0	2.9	−190	3.68	–
Xe/Cu(110), 2 × 2 unit cells	−265.4[56.2]	2.9		−30.5 [5.6]	3.8		−163.4 [5.3]	3.6		–	3.3	–
Xe/Pt(111),1/4 monolayer	−301.0[51.4]	3.0		−31.9 [5.0]	3.8		−240.2 [6.9]	3.7		–	–	–
Kr/Pt(111), monolayer	−184.7[21.1]	3.2	5.6	−24.2 [0.5]	4.2	1.4	−193.1 [3.3]	3.9	4.1	−161	–	3.9

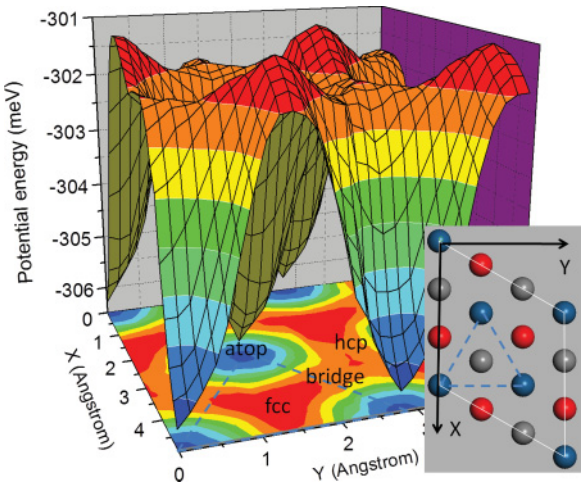

FIG. 2. (Color) The 2D potential energy surface of Xe/Pt(111) calculated from the vdW-DF2 functional. The inset is a top-down view of the (111) surface, where the blue, red, and gray balls represent atop, hcp, and fcc sites, respectively.

vdW-DF2 are a few milli-electron-volts. Thus the differences in E_{ad} between atop and hollow sites cannot account for the experimental observation of only atop site adsorption. One would expect to observe some hollow sites being occupied at the experimental temperature of 80 K with an energy difference of only a few milli-electron-volts. The only experimental data of which we are aware that probes the corrugation of the rare gas-metal surface is from Ellis *et al.*,[30] who reported a value of 9.6 meV for Xe on Pt(111) at low coverage. This can be compared with our 1/4 monolayer Xe/Pt(111) calculation (Table I) of 6.9 meV. This reasonably good agreement with experiments gives confidence in our vdW-DF2 calculations.

Examination of the 2D PES for $(\sqrt{3}\times\sqrt{3})R30^{\circ}$ Xe/Pt(111) shows why hollow site occupation is not experimentally observed. We have used PBE, LDA, and vdW-DF2 to compute the 2D PES for Xe/Pt(111). The vdW-DF2 PES is shown in Fig. 2. We classify the atop and bridge sites through examination of the PES as the global minimum and an index 1 saddle point, respectively; the fcc and hcp sites are index 2 saddle points. The eigenvectors for Xe on the atop, bridge, and fcc/hcp sites have 0, 1, and 2 imaginary frequencies, respectively, as computed from all three functionals. It is remarkable that three very different functionals give qualitatively similar PESs, but for very different reasons (*vide infra*). This consistency indicates that the general characteristics of the PES are not sensitive to the DFT functional. Furthermore, using LJ potentials for Pt and Xe gives qualitatively similar results, but with the atop site being a saddle point of index 2 and the hollow sites being the only minima on the PES. Another way to interpret the PES is that the threefold symmetry of the atop and hollow sites require that these sites be either minima or saddle points of index 2. For weakly bound systems, when one site (atop or hollow) is the energy minimum, the other site (hollow or atop) must be a saddle point and thus not easily observable in experiments. This is because weakly bound systems cannot exhibit the very high corrugation of the PES associated with chemical binding.

The question of why the low-coordination sites are minima on the PES can be addressed through decomposition of the total DFT energy into exchange, correlation, kinetic, electrostatic, and nonlocal-vdW interactions. Our LDA calculations agree with those of Da Silva *et al.*[16,17] showing that at the calculated LDA equilibrium distance of $d = 3.2$ Å the exchange energy at the atop site is lower than at the fcc site by about 31.1 meV. This is the main contribution to the atop site being energetically favored within LDA, which lead Da Silva and co-workers to identify weaker Pauli repulsion at atop sites as the reason for the larger binding energy compared with hollow sites. In contrast, at the vdW-DF2 equilibrium distance of $d = 3.8$ Å the exchange energy favors the fcc rather than atop site by $\approx$3.4 meV. Hence we conclude that the LDA functional gives a qualitatively correct PES, but for the wrong reason, since exchange repulsion is actually not weaker for the atop site at the correct equilibrium distance. The contributions of the local correlation energy favor atop site over fcc site by about 0.9 meV with vdW-DF2. Nonlocal dispersion interactions favor the high-coordination fcc site as expected, but only by $\approx$0.4 meV, so the nonlocal vdW contribution plays essentially no role in the site preference. It does, however, play a crucial role in determining the correct equilibrium distance and the scale of the PES. Decomposition of interaction energies into kinetic and electrostatic terms (obtained using ABINIT[31,32]) show that the site preference is dictated by a delicate balance between the kinetic energy and the electrostatic energy; the atop site has a lower kinetic energy than the fcc site by $\approx$50 meV, while the electrostatic energy is higher at the atop site by 43 meV. Therefore, the kinetic + electrostatic energies favor atop over fcc sites by about 7 meV (this value is close to 7.9 meV obtained from VASP calculations, indicating good agreement between ABINIT and VASP calculations).

A close look at the charge density difference shows that the potential energy pathway from the atop to the fcc sites is influenced by the hybridization between the $5p$ electrons of Xe and d electrons of Pt. Figure 3 shows the charge density difference isosurface between $(\sqrt{3}\times\sqrt{3})R30^{\circ}$ Xe/Pt(111) and the clean Pt(111) surface combined with the Xe monolayer ($\rho^{\mathrm{diff}} = \rho^{\mathrm{Xe/Pt}} - \rho^{\mathrm{Pt}} - \rho^{\mathrm{Xe}}$), at four points on the line between the atop and fcc sites. We see that the charge density difference changes gradually from atop to fcc sites, with the hybridization between the $5p$ electrons of Xe and d electrons of Pt being stronger at the atop site and decreasing continuously along

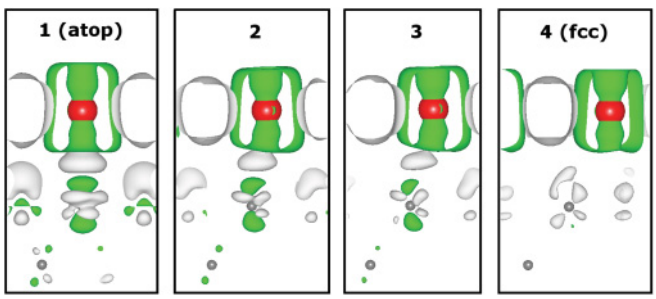

FIG. 3. (Color online) Charge density difference isosurfaces for Xe/Pt(111) computed from the PBE functional for four configurations along the path from the atop to the fcc site. The light gray and green (gray) colors represent the 1.5×10^{-4} and -1.5×10^{-4} $e/\text{Å}^3$ isosurfaces, respectively. Xenon is shown as the red (black) circle in each panel.

the path from atop to fcc. This agrees well with the energy decomposition, because increased hybridization between the orbitals decreases the kinetic energy at the atop site, and results in a lower adsorption energy compared to the hollow site.

After submitting this paper we became aware of work by Zhang *et al.*[33] who computed the 2D PES for Ne and Kr on Pb(111) using both LDA and vdW-DF. Their work shows that the atop sites are maxima and the hollow sites are minima. Their findings are consistent with our observations that it is the interaction between *p* electrons of the rare gas atoms and the *d* electrons of the transition metal surfaces that is critical in making the atop site the minimum. Hollow sites are preferred for Pb(111) because the Pb *d* orbitals are filled.

The data in Table I indicate that the preference for noble gases to adsorb at low-coordination sites is quite general, even extending to the non-close-packed Xe/Cu(110) system. In all cases the energy differences between the high- and low-coordination sites are a few milli-electron-volts as computed from vdW-DF2. For all of these systems, our calculations show that the low-coordination sites are minima and the high-coordination sites are maxima on the 2D PES. *Thus, the finding that the experimentally observed adsorption site preference is dictated by the presence of high-index saddle points rather than strong energetic differences between competing adsorption sites is a fairly general phenomenon.*

We thank L. W. Bruch, R. D. Diehl, and K. D. Jordan for helpful discussions. This work was performed in support of the National Energy Technology Laboratory's ongoing research in the area of carbon management under the RDS Contract DE-AC26-04NT41817. Calculations were performed at the University of Pittsburgh Center for Simulation and Modeling.

*karlj@pitt.edu

[1] G. Vidali, G. Ihm, H.-Y. Kim, and M. W. Cole, Surf. Sci. Rep. **12**, 135 (1991).
[2] L. W. Bruch, R. D. Diehl, and J. A. Venables, Rev. Mod. Phys. **79**, 1381 (2007).
[3] R. D. Diehl, T. Seyller, M. Caragiu, G. S. Leatherman, N. Ferralis, K. Pussi, P. Kaukasoina, and M. Lindroos, J. Phys. Condens. Matter **16**, S2839 (2004).
[4] M. Potthoff, G. Hilgers, N. Müller, U. Heinzmann, L. Haunert, J. Braun, and G. Borstel, Surf. Sci. **322**, 193 (1995).
[5] G. Hilgers, M. Potthoff, N. Müller, and U. Heinzmann, Surf. Sci. **322**, 207 (1995).
[6] J. M. Gottlieb, Phys. Rev. B **42**, 5377 (1990).
[7] L. W. Bruch, A. P. Graham, and J. P. Toennies, Mol. Phys. **95**, 579 (1998).
[8] M. Caragiu, T. Seyller, and R. D. Diehl, Phys. Rev. B **66**, 195411 (2002).
[9] T. Seyller, M. Caragiu, R. D. Diehl, P. Kaukasoina, and M. Lindroos, Chem. Phys. Lett. **291**, 567 (1998).
[10] B. Narloch and D. Menzel, Chem. Phys. Lett. **270**, 163 (1997).
[11] M. Caragiu, T. Seyller, and R. D. Diehl, Surf. Sci. **539**, 165 (2003).
[12] L. W. Bruch, M. W. Cole, and E. Zaremba, *Physical Adsorption: Forces and Phenomena* (Oxford University Press, New York, 1997).
[13] J. R. Cerdá, P. L. de Andres, F. Flores, and R. Perez, Phys. Rev. B **45**, 8721 (1992).
[14] R. O. Jones and O. Gunnarsson, Rev. Mod. Phys. **61**, 689 (1989).
[15] J. E. Müller, Phys. Rev. Lett. **65**, 3021 (1990).
[16] J. L. F. Da Silva, C. Stampfl, and M. Scheffler, Phys. Rev. Lett. **90**, 066104 (2003).
[17] J. L. F. Da Silva, C. Stampfl, and M. Scheffler, Phys. Rev. B **72**, 075424 (2005).
[18] J. L. F. Da Silva and C. Stampfl, Phys. Rev. B **77**, 045401 (2008).
[19] M. Dion, H. Rydberg, E. Schröder, D. C. Langreth, and B. I. Lundqvist, Phys. Rev. Lett. **92**, 246401 (2004).
[20] K. Lee, É. D. Murray, L. Kong, B. I. Lundqvist, and D. C. Langreth, Phys. Rev. B **82**, 081101 (2010).
[21] J. Wellendorff, A. Kelkkanen, J. J. Mortensen, B. I. Lundqvist, and T. Bligaard, Top. Catal. **53**, 378 (2010).
[22] A. K. Kelkkanen, B. I. Lundqvist, and J. K. Nørskov, Phys. Rev. B **83**, 113401 (2011).
[23] T. Seyller, M. Caragiu, R. D. Diehl, P. Kaukasoina, and M. Lindroos, Phys. Rev. B **60**, 11084 (1999).
[24] G. Román-Pérez and J. M. Soler, Phys. Rev. Lett. **103**, 096102 (2009).
[25] J. P. Perdew, K. Burke, and M. Ernzerhof, Phys. Rev. Lett. **77**, 3865 (1996).
[26] G. Kresse and J. Furthmüller, Phys. Rev. B **54**, 11169 (1996).
[27] W. Widdra, P. Trischberger, W. Frieß, D. Menzel, S. H. Payne, and H. J. Kreuzer, Phys. Rev. B **57**, 4111 (1998).
[28] D. L. Meixner and S. M. George, Surf. Sci. **297**, 27 (1993).
[29] B. Hall, D. L. Mills, P. Zeppenfeld, K. Kern, U. Becher, and G. Comsa, Phys. Rev. B **40**, 6326 (1989).
[30] J. Ellis, A. P. Graham, and J. P. Toennies, Phys. Rev. Lett. **82**, 5072 (1999).
[31] X. Gonze, J.-M. Beuken, R. Cara-cas, F. Detraux, M. Fuchs, G.-M. Rignanese, L. Sindic, M. Verstraete, G. Zerah, F. Jollet, M. Torrent, A. Roy, M. Mikami, P. Ghosez, J. Y. Raty, and D. C. Allan, Comput. Mater. Sci. **25**, 478 (2002).
[32] ABINIT was used for energy decomposition because it is not convenient to do this analysis within VASP.
[33] Y. N. Zhang, F. Hanke, V. Bortolani, M. Persson, and R. Q. Wu, Phys. Rev. Lett. **106**, 236103 (2011).